Industrial Chemistry & Materials

ROYAL SOCIETY OF CHEMISTRY

MINI REVIEW

View Article Online
View Journal | View Issue

Cite this: *Ind. Chem. Mater.*, 2023, **1**, 486

Recent progress in high-loading single-atom catalysts and their applications

Jiahui Luo,[ab] Geoffrey I. N. Waterhouse,[c] Lishan Peng *[ab] and Qingjun Chen *[ab]

Single-atom catalysts (SACs) attract significant attention owing to their high catalytic activity, high metal atom utilization efficiency, and well-defined and configurable active sites. However, achieving single-atom dispersion of active metals at high metal loadings remains challenging, limiting the performance of SACs in many practical applications. Herein, we provide a comprehensive review of recent methods developed for synthesizing high-loading SACs, critically exploring their advantages, limitations, and wider applicability. Additionally, we showcase the benefits of high-loading SACs in the oxygen reduction reaction (ORR), water electrolysis, photocatalytic hydrogen production and CO oxidation. Although great recent progress has been made in the synthesis of high loading SACs, simple and universal routes that allowed the pre-programmed preparation of single metal and multi-metal SACs with specific metal coordination need to be discovered.

Received 13th June 2023,
Accepted 24th August 2023

DOI: 10.1039/d3im00062a

rsc.li/icm

Keywords: Single atom catalyst; High-loading; Synthesis methods; ORR; Water electrolysis; CO oxidation.

1 Introduction

In recent years, single-atom catalysts (SACs) have attracted considerable attention in the field of heterogeneous catalysis due to their efficient metal utilization, adjustable active sites, and unique catalytic properties, thereby offering great potential for future application in the chemical industry and energy sector.[1–5] As early as 2011, Zhang and his collaborators[6] put forward the concept of SACs for the first time. Since that time, SACs have increasingly become the

[a] *Key Laboratory of Rare Earths, Chinese Academy of Sciences, Ganjiang Innovation Academy, Chinese Academy of Sciences, Ganzhou 341000, China. E-mail: lspeng@gia.cas.cn, qjchen@gia.cas.cn*
[b] *School of Rare Earths, University of Science and Technology of China, Hefei 230026, P. R. China*
[c] *School of Chemical Sciences, The University of Auckland, Auckland 1142, New Zealand*

Jiahui Luo

Jiahui Luo received her B.E. degree from Central South University of Metallurgical Engineering in 2021. She is pursuing her M.E. degree in Ganjiang Innovation Academy, Chinese Academy of Sciences under the supervision of Prof. Lishan Peng and Qingjun Chen. Her current research interest focuses on electrocatalysts for the oxygen reduction reaction

Lishan Peng

Lishan Peng is currently an associate professor in the Ganjiang Innovation Academy, Chinese Academy of Sciences. He obtained his Ph.D. degree in chemical engineering and technology in 2019 from Chongqing University. Subsequently he worked as a postdoctoral researcher in the Westlake University, the University of Auckland (UoA, New Zealand) and the Technical Institute of Physics and Chemistry, Chinese Academy of Sciences. His research interests focus on the design and theoretical study of advanced electrocatalysts for energy storage and conversion, such as water splitting, H_2-fuel cells, and metal–air batteries

focus of research in the fields of electrocatalysis, thermal catalysis and photocatalysis.[7–9] SACs have many advantages over traditional metal nanoparticle-based catalysts. Firstly, their active sites, which typically consist of a metal atom coordinated by 2–5 heteroatoms (N, O, S, B or P) on a support, can be pre-programmed, allowing researchers to explore reaction mechanisms at the molecular level. Secondly, SACs have very high metal atom utilization efficiency (~100% in some cases) and ultra-high reactivity, surpassing the performance of metal nanoparticle-based catalysts on both counts.[10] Many studies have shown that SACs are significantly more active than their nanoparticle counterparts.[11–15] For the above reasons, SACs have become a main focus of many research groups, leading to rapid advancements in the field in the past few years.[16] For example, Xin and coworkers[17] recently used dissolution and carbonization methods to synthesize/characterize monometallic SACs for 37 different metal elements, establishing the largest SAC library reported to date. This work is significant as it allows benchmarking of SACs for different applications, guiding rational improvements in catalyst design.

In SACs, single atoms are very active and have high surface free energies.[18] Accordingly, to stabilize the atomically dispersed metals against aggregation, the local coordination of the metal atoms is important. Most studies to date relating to SACs utilize N-doped carbon supports, with the isolated metal atoms typically having MN_4, MN_3 or MN_2 first coordination shells. Such SACs are typically prepared by pyrolysis routes using metal salts and nitrogen/carbon-rich precursors, with the metal contents generally kept low in order to avoid metal agglomeration into nanoparticles. This limits the SAC loading in the derived M_1–N–C catalysts to typically a low weight percent. Such low active site densities lead to low overall catalyst activity in industrial applications.[19–21] For example, Sa *et al.* reported a "silica protective layer-assisted" strategy that effectively prevented the aggregation of Fe atoms during high-temperature pyrolysis synthesis of Fe_1–N–C catalysts. However, due to the low loading of Fe as the active centre (1.9 wt%), the overall performance of the catalyst was not greatly improved.[22] Researchers are now targeting high-loading SACs with metal loadings >5 wt%, aiming to significantly boost the overall activity of the catalyst through increasing the number of available active sites.[23] Table 1 summarizes recent research towards high-loading SACs for specific applications, with most studies realizing a metal loading greater than 5 wt%.

A further advantage of preparing high-loading SACs is synergistic effects between adjacent metal atoms, which can have a dramatic effect on catalytic activity and selectivity.[24,25]

Electronic and spin interactions between nearby atomically dispersed metal atoms can modulate and enhance SAC performance, stimulating new research into dual metal single atoms catalysts. An overarching goal of current SAC research is the discovery of novel synthetic strategies for the preparation of high-loading SACs with high activity, selectivity, and stability (in particular suppressing metal agglomeration).[26,27] At the same time, improved understanding of the structural and catalytic properties of SACs at the atomic and molecular scales is needed.[28–30]

In this review, we discuss and summarize the main synthesis methods used to prepare high-loading SACs, such as pyrolysis methods, wet chemistry methods, electrochemical methods, atomic layer deposition (ALD) method, and so forth. Then we explore how the adjustment of some specific parameters in these classic synthesis methods enables the synthesis of high-loading SACs.[48,49] The review then explores some important applications of high-loading SACs, including the oxygen reduction reaction (ORR), water electrolysis, photocatalytic hydrogen generation, CO oxidation, and other catalytic reactions. Finally, the challenges and future prospects of high-loading SACs in industrial catalytic applications are examined.

2 Synthetic methods towards high-loading SACs

The synthesis of SACs requires care to avoid metal agglomeration as much as possible.[50,51] The dispersion or agglomeration of metal atoms involves competition between the relative strengths of the metal–support interactions and metal–metal bonds.[41] The nature of the support and its affinity for particular metals are therefore vital to realizing SACs with high-loadings. A strong metal–support interaction is vital to achieving a high metal atom loading and for enhancing catalytic activity.[52,53] The main purpose of this section is to provide an overview of the different synthesis methods commonly used to prepare SACs and then to explore whether these methods can be modified for the synthesis of high-loading SACs.

Qingjun Chen

Qingjun Chen received his Ph.D from East China University of Science and Technology in 2012. After that, he worked as an assistant professor in Shanghai Advanced Research Institute, Chinese Academy of Sciences. From 2013 to 2021, he continued his research as a postdoc/researcher/professor in the University of Toyama (Japan), Norwegian University of Science and Technology (NTNU, Norway), and Institute of Process Engineering, Chinese Academy of Sciences, successively. Since 2021, he has been a professor at the Ganjiang Innovation Academy, Chinese Academy of Sciences. His research interests are hydrogen energy and fuel cells.

Table 1 Summary of recently reported high-loading single atom catalysts (SACs)

Atomically dispersed metal atom	Catalyst	Metal loading (at%)	Metal loading (wt%)	Synthesis method	Application
Pt	Pt/meso S–C (ref. 31)	~0.68	10.0	Pyrolysis method, wet chemical method	Catalytic hydrogenation of quinoline, electrochemical oxidation formic acid
Pt	Pt–N–C (ref. 32)	~2.85	32.3	Pyrolysis method	—
Pt	Pt SAC[33]	~0.58	8.7	Facile ion exchange method, pyrolysis method	Photocatalytic hydrogen evolution reaction
Pt	Pt SAC[34]	~0.83	12.0	Pyrolysis method	Photocatalytic H_2 evolution
Pt	Pt/Co_3O_4 (ref. 24)	1.1	6	Pyrolysis method	Water electrolysis
Pt	$Pt_1/Co(OH)_2$ (ref. 35)	1.9	—	Electrochemical method	Water electrolysis (hydrogen evolution reaction)
Ir	Ir/meso S–C (ref. 31)	~0.69	10.0	Pyrolysis method, wet chemical method	Catalytic hydrogenation of quinoline, electrochemical oxidation of formic acid
Ir	$Ir(CO)_2$/rGA[36]	~1.07	14.8	Coprecipitation method	Hydrazine electrooxidation
Ir	Ir–N–C (ref. 32)	3.84	41.6	Pyrolysis method	—
Ir	$Ir_1/Co(OH)_2$ (ref. 35)	2.6	—	Electrochemical method	Water electrolysis (oxygen evolution reaction)
Cu	Cu–N–C (ref. 37)	~4.75	20.9	Pyrolysis method	Oxygen reduction reaction
Fe	Fe–NC SAC[38]	1.09	8.9	Pyrolysis method	Oxygen reduction reaction
Mo	Mo SAC[39]	~1.30	9.54	Pyrolysis method	Electrocatalytic N_2 reduction reaction
Fe	Fe-SAC[40]	0.98	7.7	Pyrolysis method	Oxygen reduction reaction
Fe	$FeN_X/g\text{-}C_3N_4$ (ref. 41)	~4.55	18.2	Pyrolysis method	Organic pollutant degradation
Fe	FeSA-NGK[42]	~3.43	14.2	Thermal oxidation calcination method	Advanced oxidation processes (AOP) for BPA degradation
Fe	Fe SAC[43]	~1.07	4.8	Pyrolysis method	Oxygen reduction reaction
Fe	Fe–NC (ref. 44)	~1.59	7	Pyrolysis method	Oxygen reduction reaction
Co	Co–NC SAC[38]	~2.72	12.1	Pyrolysis method	Oxygen reduction reaction
Ni	Ni-SAC[45]	~1.13	5.3	Pyrolysis method	CO_2 reduction reaction
Ni	NiSA-N-CNT[46]	~4.93	20.3	Pyrolysis method	CO_2 reduction reaction
Ni	Ni–N–C (ref. 32)	3.6	15.4	Pyrolysis method	CO_2 reduction reaction
Zn	Zn–N–C (ref. 47)	~1.86	9.33	Pyrolysis method	Oxygen reduction reaction

2.1 Pyrolysis methods

Pyrolysis methods are widely used for SAC synthesis (especially M_1–N–C catalysts), with precursor heating under an inert atmosphere creating N–C catalysts with sites for immobilizing metal atoms. However, during the pyrolysis process, metal atoms are highly susceptible to agglomerate to form nanoparticles, with post-synthetic treatments in acid often used to selectively dissolve the metal nanoparticles to leave only SACs.[43] How to effectively design precursors to achieve physical or chemical confinement of metal atoms and avoid laborious post-synthetic treatments is an important challenge for the preparation of high-loading SACs.[32,42,54,55]

The use of metal–organic frameworks (MOFs) as precursors allows the synthesis of SACs with spatially separated metal sites, tunable structures, and flexible coordination geometries. For example, Qiao *et al.* revealed the formation mechanism of high-density single atoms with electronic metal–metal interactions using *in situ* spectroscopy characterization studies and theoretical calculations.[24] Using ZIF-67 as a starting material, they discovered that high-density Pt ions could be embedded into the ZIF-67 skeleton through ion exchange with Co to form Pt–N coordination sites. This process was in line with the hard and soft acid–base theory (HSAB), which states that ion exchange can occur when the acid–base interaction between the introduced metal and ligand is stronger than the host metal–ligand interaction. During the subsequent pyrolysis process, the Pt–N bond in the first shell breaks at lower temperatures and evolves into a Pt–O–Pt coordination, followed by Co–N cleavage to form Co–O, which promotes the formation of high-density Pt SACs on a Co_3O_4 support (Pt loadings up to 6 wt% or 1.1 at%) with Pt–Pt interactions between adjacent Pt atoms. The SAC loading achieved was higher than most reported Pt-based ORR catalysts. In addition, Sun *et al.* prepared a layered g-C_3N_4 carrier (NGK) from kaolin by thermal oxidation calcination.[42] Subsequently, Fe ions were assembled into the "sixfold cavities" of NGK through high-temperature treatment, allowing Fe atoms to combine with N atoms and form a stable atomic structure, as shown in Fig. 1a. Through

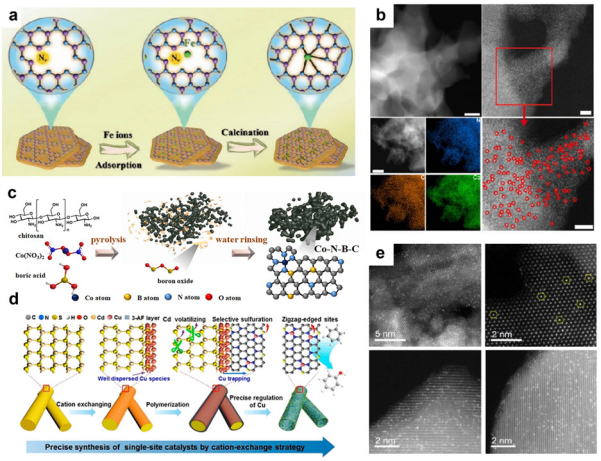

Fig. 1 (a) Schematic diagram for preparation of high-loading Fe SACs by pyrolysis. Reprinted with permission from ref. 42. Copyright 2022, Wiley-VCH GmbH; (b) STEM and EDX electron microscopy images of Co SACs with 23.58 wt% load obtained by pyrolysis. Reprinted with permission from ref. 57. Copyright 2023, Springer Nature; (c) Schematic diagram of a novel boric acid assisted pyrolysis strategy for producing SACs with abundant edge defects and high loading. Reprinted with permission from ref. 56. Copyright 2023, Wiley-VCH GmbH; (d) Schematic diagram of SACs prepared by cation exchange for sulfur–nitrogen dicoordination. Reprinted with permission from ref. 58. Copyright 2020, American Chemical Society; (e) Electron microscopy of the Pt_1/FeO_x catalyst prepared by the coprecipitation method. Reprinted with permission from ref. 59. Copyright 2019, Springer Nature.

introducing kaolinite, g-C_3N_4 and nitrogen vacancies, the anchoring efficiency of Fe single atoms was enhanced, thus avoiding Fe agglomeration. Thanks to the carrier effect of kaolinite, the load of Fe single atoms was successfully increased to 14.2 wt% (~3.4 at%). The obtained Fe single-atom composite (Fe SA-NGK) possessed high catalytic activity for the ORR.

To prepare edge-defect-rich high-loading Co SACs, Xu *et al.* developed a boric acid-assisted pyrolysis strategy (Fig. 1c).[56] Using chitosan, cobalt nitrate, and boric acid as precursors, a Co–N–B–C catalyst rich in exposed sheet edges and with high Co loadings was synthesized by a one-step pyrolysis method. During pyrolysis, B_2O_3 was formed by the dehydration of boric acid. Since the temperature in the pyrolysis was much higher than the melting point of B_2O_3, B_2O_3 remained in a liquid state. Chitosan carbonization thus occurred within the molten B_2O_3 medium, yielding a N-doped carbon skeleton with abundant pores and rich in edge defects after washing to remove B_2O_3. The use of molten B_2O_3 was very effective in preventing Co single atoms from agglomerating. The reported Co monoatomic loading was 4.2 wt% (~0.9 at%), though it is expected that much higher Co SA loadings could be achieved by optimization of this novel method. To further improve the loading of Co SAs, Wang *et al.* mixed dicyandiamide, formaldehyde, and $Co(NO_3)_2{\cdot}6H_2O$ in distilled water, stirred them vigorously, then heated the mixture at 100 °C for more than 12 h to completely evaporate the solvent.[57] In this process, formaldehyde and dicyandiamide were polymerized, whilst Co ions were fully coordinated by the obtained dicyandiamide–formaldehyde resin. The purple solid was then heated in a tubular furnace to 600 °C under Ar and held at that temperature for 2 h, then cooled to room temperature and heated to 400 °C in a H_2/Ar (5%) atmosphere for 2 h. The Co SAC prepared by this method had a remarkable Co loading of 23.58 wt% (~5.9 at%) and very uniform Co dispersion (Fig. 1b), representing a notable breakthrough in the synthesis of high-loading SACs.

Nowadays, pyrolysis methods remain very popular for synthesizing SACs due to their simplicity. The above examples demonstrate that by judicious selection of precursors and pyrolysis parameters, it is possible to reduce metal agglomeration and greatly increase the overall loading of atomically dispersed metals. Pyrolysis is likely to remain one of the most important methods for the synthesis of high-loading SACs in the future.

2.2 Wet chemical methods

Among traditional methods used for SAC synthesis, wet chemical methods are indispensable (especially in the field of catalysis) due to their simple operation and the possibility of mass production. Wet methods include coprecipitation methods, impregnation methods, and ion exchange methods, amongst others. Generally, these methods consist of the following steps:

i) The metal precursor is attached to the surface of a carrier through impregnation, adsorption, ion exchange, co-precipitation, or other methods;

ii) The modified carrier is dried or heat treated (sometimes this step can be omitted);

iii) Reduction or activation.

Generally, the reaction conditions used in wet chemical methods are mild and more easily controlled compared to those of pyrolysis methods. However, many parameters in the preparation process influence the performance of the obtained SACs. The parameters need to be strictly controlled, including the addition speed of the precursor, stirring speed, reaction temperature, reaction time, reduction/activation conditions, *etc.* In addition, some metal atoms loaded onto the carrier may aggregate, making it difficult for them to be transformed into single atoms. High-loading SACs are generally difficult to prepare using wet methods.

In 2020, Wu *et al.* prepared a kind of metal (M) centered catalyst (M = Cu, Pt, Pd, *etc.*) with sulfur (S) and nitrogen (N) coordination by cation exchange (Fig. 1d).[58] The synthesis method involved converting the surface part of CdS nanorods into subnano/atomic layer Cu_2S *via* cation exchange. Then, a 3-aminophenol/formaldehyde (3-AF) layer was deposited on the CdS/Cu_2S surface and the resulting sample was heated at 900 °C under an N_2 atmosphere. The 3-AF layer was converted into a nitrogen-doped carbon (NC) shell *in situ*. Then Cd^{2+} was gradually reduced by the NC and evaporated due to the low boiling point of Cd. The volatile S species selectively vulcanized the NC. The Cu species diffused into the edge-enriched S and

N defects to form a monatomic copper catalyst. Lang *et al.* added a mixture of chloroplatinic acid and ferric nitrate into a sodium carbonate solution dropwise. *Via* this co-precipitation method, a Pt_1/FeO_x catalyst with a Pt loading up to 1.8 wt% was finally prepared.[59] As shown in Fig. 1e, Pt was uniformly dispersed on the FeO_x support in the form of single atoms. Even with heating at 800 °C, the dispersed Pt atoms were resistant to agglomeration.

The wet chemical method remains common for SAC preparation, with the SACs prepared by this method being characterized by good metal dispersion and low susceptibility to forming metal clusters. However, the loading of SACs prepared by this method is difficult to increase. Studies concerning the synthesis of high-loading SACs by the wet chemical method are still relatively rare.

2.3 Atomic layer deposition (ALD)

As an emerging technology for SAC synthesis, atomic layer deposition is a continuous self-limiting molecular-level cyclic process based on the reaction between gaseous chemical precursors and solid substrate surfaces.[60–62] It can be used for the preparation of uniform thin films, single atoms of regular dispersion, subnano clusters, and nanoparticles (NP) in porous materials. Compared with other deposition techniques such as chemical vapor deposition (CVD), physical vapor deposition (PVD), or electrochemical deposition, ALD possesses significant advantages, which are summarized as follows:[63] i) the amount of deposited metal can be accurately controlled; ii) metal atoms are evenly dispersed; iii) the method exhibits surface chemical selectivity; iv) the method can be scaled and applied industrially.

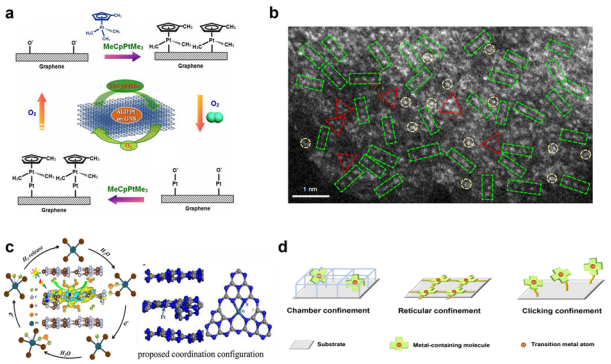

Fig. 2 (a) Schematic diagram of deposition of Pt by atomic layer deposition. Reprinted with permission from ref. 64. Copyright 2013, Springer Nature; (b) High-resolution HAADF-STEM image of $Ni_1Cu_2/g\text{-}C_3N_4$, where isolated atoms, triangular trimers and linear trimers are represented by yellow circles, red triangles and green rectangles, respectively. Reprinted with permission from ref. 65. Copyright 2021, Springer Nature; (c) Schematic diagram of Pt SAC and restricted Pt single-atom coordination structures prepared by an interlayer nano-space confinement strategy. Reprinted with permission from ref. 33. Copyright 2020, Elsevier; (d) Schematic diagram of three different limiting strategies (chamber-limited strategy, lattice-limited strategy and click-limited strategy). Reprinted with permission from ref. 69. Copyright 2022, American Association for the Advancement of Science.

In an early study, Sun *et al.* used (methylcyclopentadienyl)-trimethyl platinum as the precursor to deposit platinum on a graphene carrier *via* ALD under nitrogen purging (Fig. 2a).[64] During the oxidative decomposition of $MeCpPtMe_3$, some precursor ligands reacted with surface adsorbed oxygen to form CO_2, H_2O, and hydrocarbon fragments. This provided a self-limiting growth energy sufficient to construct a platinum-containing monolayer during ALD. More oxygen adsorbed on the Pt surface to form a new adsorbed oxygen layer, thus completing an ALD cycle. By this approach, the amount of Pt deposition could be accurately controlled by adjusting the number of ALD cycles. The average size of Pt particles on graphene was 0.5, 1–2, and 2–4 nm for 50, 100, and 150 ALD cycles, respectively. Pt loading on graphene was 1.52 wt% (~0.09 at%), 2.67 wt% (~0.17 at%) and 10.5 wt% (~0.72 at%), respectively. In these samples, Pt co-existed in the form of single atoms, small Pt clusters, and Pt NPs. Gu *et al.* adopted atomic layer deposition (ALD) to deposit monatomic copper and nickel on a carrier (Fig. 2b).[65] The developed experimental method involved first making an atomic copper "gripper" on $g\text{-}C_3N_4$ by Cu ALD (also known as $Cu_1/g\text{-}C_3N_4$), where the saturation Cu loading was about 11.2 wt%. Subsequently, $Ni_yCu_1/g\text{-}C_3N_4$ (y is the atomic ratio of Ni to Cu) was synthesized by depositing Ni atoms on subsaturated $Cu_1/g\text{-}C_3N_4$ by NiO_x ALD. It was shown that the Ni loading decreased with increasing Cu loading, demonstrating that open N_{py} sites together with adjacent Cu atoms provide anchoring sites for guest atoms (*i.e.* Ni) at subsaturation Cu coverage, similar to chelating ligands in organometallic chemistry. Using this approach, a compact atomic copper "gripper" (8.1 wt%/~0.17 at%) on $g\text{-}C_3N_4$ was used to stabilize a relatively high-loading of monatomic nickel catalyst (3.1 wt%/~0.65 at%). Thanks to the atomic layer deposition method and the metal–carrier interaction, SACs with high metal loadings were obtained.

To sum up, ALD is an emerging technology for the synthesis of SACs, clusters, and nanoparticle catalysts. It is expected to play an increasingly important role in the preparation of high-loading SACs for different applications in the future.

2.4 Electrochemical methods

Compared with thermochemical methods, electrochemical methods represent a milder, more environment-friendly and energy-efficient route towards high-loading SACs. Generally, electrochemical syntheses of SACs are carried out at near ambient temperature and pressure. Also, the synthesis parameters can be fine-tuned by changing the input electrochemical technique (*e.g.*, linear sweep or cyclic voltammetry, CV) or by continuously adjusting the applied current, voltage, sweep rate, and reaction time to obtain the desired product. For these reasons, electrochemical methods have recently attracted intense interest from the research community.

Tavakkoli *et al.* used bulk Pt foils and single-walled carbon nanotubes (SWCNTS) coated on glassy carbon electrodes as counter electrodes and working electrodes, respectively, to electrochemically deposit Pt atoms onto SWCNTS through a continuous voltage cycle.[66] By this electrodeposition approach, Pt atoms could be immobilized on carbon nanotubes or graphite. In addition, Pt SACs on CoP-based nanotube arrays (supported on nickel foam) were successfully prepared by controlled potential cycling.[67] Zhang *et al.* used a standard three-electrode system to grow $Co(OH)_2$ nanosheets on a glassy carbon working electrode.[68] By adding a low concentration of $IrCl_4$ to 1 M KOH electrolyte, a C–Ir_1/$Co(OH)_2$ catalyst was successfully obtained over ten scanning cycles. The monatomic Ir was evenly dispersed on the $Co(OH)_2$ substrate, with the mass loading of Ir around 2.0 wt%, verified by inductively coupled plasma atomic emission spectrometry (ICP-AES).

Electrochemical methods represent a relatively new SAC synthesis method, being both simple and easily controllable. However, similar to wet chemical methods, achieving high single atom loadings remains challenging, motivating the search for improved synthetic methodologies.

2.5 Other methods

In addition to the methods discussed above, there are many other methods now being used to prepare SACs, including electrospinning, ion exchange, click chemistry, mass-selected soft-landing methods, and so on.[48]

Quan's team reported an interlayer nano spatial restriction strategy in 2019 for the first time (Fig. 2c).[33] A simple electrostatic ion exchange method was used to embed potassium ions into graphitic carbon nitride (g-C_3N_4–K). Then, the prepared g-C_3N_4–K was mixed with $Pt(NH_3)_4Cl_2$ solution to load Pt onto the surface of the material. Here, the negatively charged g-C_3N_4–K induced the spontaneous adsorption of Pt ions *via* electrostatic attraction. Through ion exchange with K^+, Pt ions were inserted into the interlayer nanospace and confined by the adjacent layers. Finally, the obtained yellow powder was heated in an Ar atmosphere to enhance the interaction between Pt atoms and the support. The loading of Pt could be controlled by adjusting the amount of $Pt(NH_3)_4Cl_2$ solution used in the synthesis, with the maximum loading of Pt single atoms reaching 10.4 wt% (~0.71 at%).

The click chemistry-limited strategy devised by Zhao *et al.* differs from conventional chamber-limited and lattice-limited strategies (Fig. 2d) in that not only does it ignore strict molecular size effects or symmetry requirements, it also facilitates the controlled and directed synthesis of catalysts.[69] The authors successfully prepared Co–N–C SACs by clicking cobalt porphyrin units onto conducting substrates *via* amination reactions. Under the guidance of click chemistry, metal-containing complexes are attached to modified substrates to ensure the effective confinement of metal atoms in terms of precursor design for the construction of single-atom sites. Considering the high reaction specificity between carboxyl and amino groups, the authors chose the amidation reaction as the click reaction to graft transition metal-containing complexes onto conducting substrates. The use of cobalt(II) *meso*-tetra(4-carboxyphenyl)porphyrin and amino functionalized carbon nanotubes (CNT amino) allowed the efficient synthesis of Co SACs. Xia *et al.* used a modified molecular fusion route to synthesize well-crystallized GQDs-NH_2 dispersions.[32] They added different volumes of $IrCl_3$ stock solution (5 mg mL^{-1}) to 30 mL of the GQDs-NH_2 dispersion (1 mg mL^{-1}), then freeze-dried the resulting dispersion. Pyrolysis of the freeze-dried product created an Ir SAC with Ir loading up to 41.6 wt% (3.84 at%). Based on that, the same method was used to prepare Ni SACs with a high atomic Ni loading amount reaching 15.4 wt% (3.6 at%).[32]

2.6 Synthesis strategies and applications for different methods

There are several strategies to achieve high-loading SACs. First, defect engineering, though constructing more diverse and dense defect sites on the surface of the carrier to capture single atoms, thereby synthesizing high-loading single atom catalysts. Second, the space limitation strategy. It rationally uses diverse porous materials (ZIF, MOFs, COFs, *etc.*) to encapsulate and anchor mononuclear metal precursors, and achieve high loading and their uniform spatial distribution. Finally, for regulating coordination sites and coordination groups on the surface of the support to capture mononuclear metal precursors, a variety of coordination sites with different coordination properties are used to regulate the coordination environment of single atoms. Different ligands can provide different electron densities and coordination forces to regulate the catalytic performance of the active site. For example, the addition of a complex can make it form coordinate covalent bonds with metal ions, and wrap the metal ions. The metal ion is fixed by providing a site for the metal ion to form a coordinate covalent bond with, so as to prevent it from further reacting with other ions or molecules, thus stabilizing the metal ion and preventing it from agglomerating or aggregating in the reaction process.

After analyzing the synthesis strategies for the preparation of SACs, different synthesis methods can successfully prepare high-loading SACs through reasonable application of these strategies, and the industrialization prospects of these methods are discussed. First, the pyrolysis method can achieve excellent atom dispersion and has shown promise in industrial applications. However, the high temperature and energy requirements can make it costlier compared to wet chemistry methods. Additionally, the scalability of high-temperature pyrolysis needs further exploration. Wet chemistry methods, such as sol–gel and impregnation techniques, have been widely used. They are relatively simple and cost-effective, making them attractive for large-scale production. However, achieving high dispersion and stability of single atoms can be challenging. The electrochemical method for preparing SACs has strong industrialization

prospects due to its advantages in terms of scalability, cost-effectiveness, and market benefits. It can be easily scaled up using conventional electrochemical cells and equipment. This allows for potential large-scale production of SACs, meeting the demands of various industrial applications. Also, the electrochemical method uses relatively low-cost and abundant metal precursors. These factors contribute to the potential cost advantage of electrochemically synthesized high-loading SACs. However, ongoing research and development efforts to address challenges and optimize synthesis parameters will be crucial in realizing the full potential of electrochemically synthesized high-loading SACs in various industrial applications. Atomic layer deposition (ALD) offers great potential for atomically precise catalysts, but the complexity of synthesis and the high cost of precursor materials and equipment may limit their industrial scalability.

Considering these, wet chemistry methods currently appear to have great industrialization prospects for SACs. They are relatively cost-effective and can be easily scaled up for mass production. However, the loading of SACs prepared by this method is difficult to increase. Studies concerning the synthesis of high-loading SACs by wet chemical methods are still relatively rare. In the actual research and application, the pyrolysis method to produce high loads of single atoms still occupies a dominant position, but it is hoped that a mild and controllable wet chemical method can be developed in the future.

3 Selected applications of high-loading SACs

3.1 Oxygen reduction reaction (ORR)

The ORR reaction is a key reaction in a number of next-generation electrochemical devices including fuel cells and metal–air batteries.[70,71] In a proton exchange membrane fuel cell (PEMFC), the design of the cathode "oxygen reduction" electrocatalyst is more challenging than the anode "hydrogen oxidation" electrocatalyst.[72] This is due to the following reasons: i) oxygen reduction is a four-electron transfer process that requires fast reaction kinetics, and its exchange current density is only 1/100th that of the anodic hydrogen oxidation reaction (a two-electron transfer process). As such, the ORR is five orders of magnitude slower than the anodic hydrogen oxidation reaction. As such, the ORR is the rate limiting step in the overall PEMFC electrocatalytic reaction; ii) the oxygen reduction process is relatively complex, involving many proton and electron transfer steps and multiple intermediates, resulting in a lower energy conversion efficiency and increased oxygen reduction overpotential. Therefore, the design and development of high-performance cathodic oxygen reduction reaction electrocatalysts is vital.[72–74] In a wide variety of electrocatalysts, high-loading SACs can enhance the catalytic activity and selectivity of the ORR compared to conventional catalysts. The unique atomic dispersion of metal atoms in SACs can improve the efficiency of oxygen reduction, leading to improved fuel cell performance and energy conversion.

Pt-nanoparticle based electrocatalysts have excellent catalytic properties and efficiencies as ORR catalysts.[4] By comparison, single-atom Pt catalysts are typically ineffective in catalyzing the breakage of O–O bonds during ORR catalysis, and thus they cannot catalyze the four-electron reduction of O_2 efficiently. At low metal loadings, Pt SACs typically favor two-electron products (H_2O_2) rather than four-electron products (H_2O).[75] Ambarish Kulkarni *et al.* mentioned that the essence of the four-electron pathway is to allow O–O bond dissociation in the adsorbed *OOH.[75] Lei Zhang concluded that when the distance between Pt atoms is greater than a few angstroms (Å), neighboring Pt single-atom sites exhibit no significant interaction.[76] In this case, each Pt single-atom site remains isolated and unsupported in ORR catalysis. When the distance between two Pt single atoms is approximately 3 Å, both oxygen atoms in *OOH can be adsorbed by these two Pt atoms, effectively stretching the O–O bond and activating its cleavage, and exhibiting superior 4-electron ORR performance. Therefore, when designing atomically dispersed Pt catalysts for 4-electron ORR electrocatalysis, achieving a high metal density is crucial.[72,75] Li *et al.* applied a photochemical solid-phase reduction method to prepare high-loading Pt SACs (3.8 wt%, ~0.24 at%).[77] The catalyst exhibited excellent HER and ORR electrocatalytic properties in acid and alkaline electrolytes. The catalyst delivered a high half-wave potential of up to 0.89 V, along with high specific mass activity and specific activity, low Tafel slope, low hydrogen peroxide yield and high stability, thus superior all-round performance compared with a commercial 20 wt% Pt/C catalyst containing platinum nanoparticles (Fig. 3a–f).

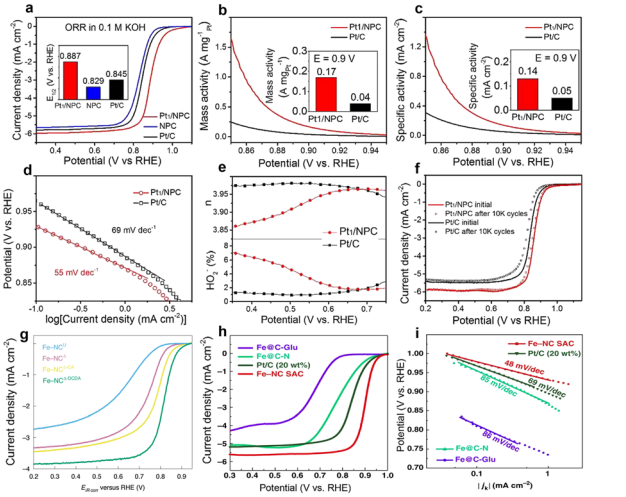

Fig. 3 (a–f) The ORR performance of single-atom platinum catalysts. Reprinted with permission from ref. 77. Copyright 2021, Elsevier; (g) The ORR activity of a single-atom Fe catalyst. Reprinted with permission from ref. 44. Copyright 2022, Springer Nature; (h and i) Steady-state ORR polarization curves and corresponding Tafel of Fe–NC SAC, Pt/C and control samples. Reprinted with permission from ref. 38. Copyright 2019, Springer Nature.

Although a high-loading Pt SAC has excellent 4-electron ORR performance, the limited reserves of Pt and its high price are obstacles to the large-scale uptake of PEMFCs. Further, supported Pt nanoparticles usually undergo agglomeration or dissolution during electrocatalytic processes, which can be highly detrimental to performance. To address these problems, researchers are now pursuing non-precious metal SACs for the ORR and other electrochemical reduction reactions that traditionally have used Pt nanoparticle-based catalysts. For example, by co-doping carbon materials with nitrogen and transition metals (TM), non-precious metal SACs with excellent electrocatalytic ORR activity can be created, serving as cathodic catalysts for proton exchange membrane fuel cells. In addition, their ORR activity can be improved by increasing the loading of TM SAC active sites. The catalytic activity of SACs depends on both the intrinsic catalytic activity and density of the active sites. In general, the intrinsic activity of TM single atom sites for a particular TM is relatively fixed, thus increasing the active site density is considered the most effective strategy for improving the catalytic activity in acidic electrolytes. Kucernak *et al.* prepared monoatomic Fe catalysts supported on N-doped carbon (Fe–NC) with a Fe loading up to 7 wt% (~1.59 at%) using a ZIF-8 precursor.[44] The presence of Fe single atoms was verified by ^{58}Fe low-temperature Mössbauer spectroscopy and Fe K-edge X-ray absorption spectroscopy, both of which demonstrated a Fe–N_4 coordination. The catalyst exhibited excellent catalytic activity for the ORR in fuel cells. Xia *et al.* prepared Ni–N–C catalysts using a self-assembly method with graphene quantum dots, achieving Ni loadings up to 15.4 wt% (3.6 at%).[32] The Ni atoms were atomically dispersed on the carrier with no agglomeration being observed. Excellent ORR activity was reported. These transition metals such as Fe, Co, Mo and Ni have been prepared to form high-loading SACs that demonstrated excellent catalytic performance for the ORR (Fig. 3g–i). Xin *et al.* prepare a high-loading Mo SAC.[39] A precursor powder containing ammonium molybdate ($(NH_4)_6Mo_7O_{24}$) and glucose was placed in a crucible and heated at 650 °C for 4 h under an Ar atmosphere. The obtained Mo SAC had a metal loading of 9.54 wt% and very good electrocatalytic properties.

In conclusion, high-loading SACs are very promising alternatives to traditional Pt nanoparticle catalysts for the ORR in PEMFCs and other applications. Much work continues, aimed at increasing the site density of single atoms on carbon supports, essential for realizing fast reaction kinetics.

3.2 Photo/electro-catalytic water splitting

Hydrogen is a promising energy carrier in the shift away from polluting fossil fuel energy. Water electrolysis using renewably generated electricity is arguably the cleanest way to manufacture hydrogen fuel at scale, with the only by-product being oxygen.[70,78] The reaction rates of the cathode hydrogen evolution reaction (HER) and anodic oxygen evolution reaction (OER) both affect the overall electrolytic water reaction efficiency. Nowadays, the main challenge of water electrolysis is to reduce the overpotentials of the HER and OER.[79] Researchers are now exploring various types of catalysts for the HER and OER in order to lower the overpotentials of these reactions. Platinum and certain precious metal oxides (RuO_2 and IrO_2) represent the benchmark HER and OER catalysts. SACs are now being pursued as lower cost alternatives to these precious metal nanoparticle-based catalysts for both the HER and OER.[80] And high-loading SACs have shown promise in improving the catalytic efficiency and stability of water splitting reactions. They can provide active and durable catalytic sites, enhancing hydrogen production and oxygen evolution kinetics.

For example, Chen *et al.* used nickel foam as the substrate and synthesized atomic ruthenium (Ru)-loaded nickel hydroxide ultrathin nanoribbons (R-NiRu) with a high atomic Ru loading amount reaching ~7.7 wt%, exhibiting a low overpotential of 16 mV for the HER at 10 mA cm^{-2} and a Tafel slope of 40 mV dec^{-1} in aqueous 1.0 m KOH solution.[81] In addition, Cheng *et al.* constructed catalysts with high-density Pt (1.9 at%) and Ir (2.6 at%) single atoms anchored on $Co(OH)_2$ by a facile one-step approach. Remarkably, $Pt_1/Co(OH)_2$ and $Ir_1/Co(OH)_2$ only required 4 and 178 mV at 10 mA cm^{-2} for the HER and OER, respectively.[35] In addition, the assembled $Pt_1/Co(OH)_2//Ir_1/Co(OH)_2$ system showed a mass activity of 4.9 A $mg_{noble\ metal}^{-1}$ at 2.0 V in an alkaline water electrolyzer, which is 316.1 times higher than that of $Pt/C//IrO_2$.

With a view towards direct solar energy conversion in hydrogen fuels, researchers are also pursuing photocatalytic hydrogen production. Zeng *et al.* constructed Pt single-atom photocatalysts with ultra-high Pt loading (8.7 wt%/~0.58 at%) using the interlayer sub-nanospace of layered carbon nitrides to confine Pt atoms.[33] Both theoretical calculations and experimental results showed that the interlayer interactions can significantly change the electronic structure of Pt atoms, causing the charge density of confined Pt atoms to change and facilitate the adsorption of protons, significantly reducing the energy barrier of photocatalytic hydrogen generation. The prepared Pt single-atom photocatalyst delivered a high photocatalytic H_2 production rate of 22 650 μmol g^{-1} h^{-1} under visible light and an apparent quantum yield (AQY) of 22.5% at 420 nm, which was much higher than most g-C_3N_4 and polymeric-based catalysts (Fig. 4a–d). In addition, it has been shown that surfactants can play an important role in the synthesis of high-loading SACs. Zhou *et al.* prepared a Pt SAC with a metal loading of 12.0 wt% (~0.83 at%) with the help of surfactants.[34] In their work, polyvinylpyrrolidone (PVP) molecules were selectively adsorbed on the surface of MOF sheets to form 2D MOF nanosheets. The prepared PtSA-MNS (ultrathin 2D MOF nanosheets coordinated with Pt single atoms) exhibited excellent photocatalytic activity for hydrogen generation under visible light and good stability (Fig. 4e and f).

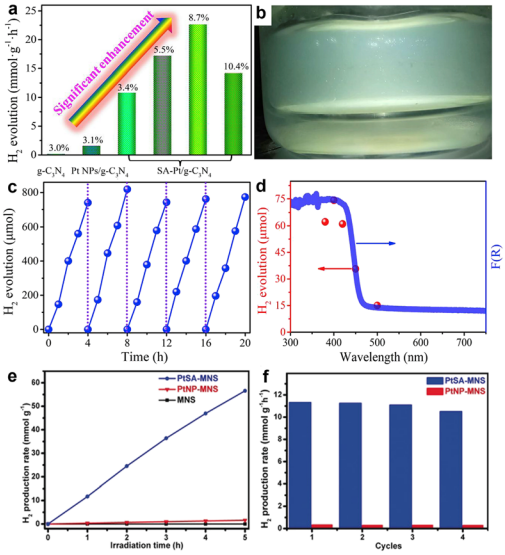

Fig. 4 (a) Visible light ($\lambda > 420$ nm) photocatalytic HER activity of g-C_3N_4, Pt NPs/g-C_3N_4-K and SA Pt/g-C_3N_4 under different Pt loads; (b) Photos of reaction using 10 mg SA Pt/g-C_3N_4-8.7; (c) Stability test and (d) SA Pt/g-C_3N_4-8.7 of the apparent quantum test. Reprinted with permission from ref. 33. Copyright 2020, Elsevier; (e and f) Characterization of photocatalytic activity, (e) photocatalytic production rates of H_2 of Pt SA MNS, Pt NP MNS and MNS and (f) cyclic stability of Pt SA MNS and Pt NP MNS. Reprinted with permission from ref. 34. Copyright 2019, Wiley-VCH GmbH.

These examples demonstrate that high-loading SACs can be beneficial for hydrogen generation *via* water electrolysis and photocatalysis, with high-loading platinum SACs showing excellent activity for both of these processes.

3.3 CO oxidation reaction

The CO oxidation reaction is an important reaction,[82] having relevance to direct methanol fuel cells, neutralization of vehicle exhaust emissions, and removal of trace amounts of CO from hydrogen-rice gas. SACs provide an ideal platform for studying the reaction mechanism of CO oxidation at a molecular level, whilst also offering the ability to greatly accelerate the CO oxidation reaction. At present, the mechanism of CO oxidation in SACs is still unclear, with catalytic elimination of carbon monoxide at room temperature still being a major challenge in the field of heterogeneous catalysis research.[83–85] Based on that, high-loading SACs can exhibit higher catalytic activity and selectivity than traditional catalysts in CO oxidation. The atomic-level dispersion of metal atoms in SACs provides efficient exposure of active sites, leading to enhanced CO oxidation performance and better tolerance to poisoning.

Pt-based catalysts have been widely studied for CO oxidation. By loading Pt single atoms on the surface of metal oxides, each Pt atom can be used as an active site for the reaction, thereby offering great advantages over Pt nanoparticle catalysts in terms of Pt atom utilization efficiency. In fuel cells, Pt nanoparticle catalysts are vulnerable to CO poisoning,[86] making the CO oxidation reaction very important. Pt SACs are not easily poisoned by CO, offering a great advantage over their nanoparticle counterparts. In traditional nanoparticle catalysts, CO molecules can bind to multiple metal atoms, inhibiting their ability to facilitate catalytic reactions. However, in Pt SACs, each metal atom is isolated and surrounded by ligands or co-catalysts, preventing CO molecules from adsorbing onto multiple metal sites. This unique atomic-level dispersion of Pt atoms reduces the probability of CO poisoning. Furthermore, the ligands or co-catalysts surrounding the Pt atoms in SACs can help stabilize the catalyst and modify its electronic structure, optimizing its activity and selectivity. This allows for enhanced catalytic performance and increased resistance to CO poisoning. Recently, Kim and his colleagues used CeO_x–TiO_2 (two-component oxides) to support a compact Pt single (or double) atom catalyst, obtaining a catalyst with excellent CO oxidation performance by adjusting the interface between the two oxide phases.[87] The CeO_x–TiO_2 interface was created by adding 1 wt% Ce on TiO_2 nanoparticles, which stabilizes Pt single-atoms by strong electronic interactions, physically disintegrates Pt into Pt-SAs and activates the interface-mediated MvK mechanism of CO oxidation, while preserving its catalytic activity against CO-poisoning. Also, the author found that the loading of Pt SACs with addition of 1 wt% of Ce to the TiO_2 support is higher than that of the TiO_2 support, resulting in superior ORR activity (Fig. 5a–c).

In order to overcome the scarcity and high cost of platinum-based catalysts, researchers are now pursuing high-performance and high-loading SACs based on earth abundant metals for CO oxidation. Zhu *et al.* systematically studied the geometric structure, electronic structure, and stability of various monatomic metals supported by oxygen functionalized Ti_2C (Ti_2CO_2) M_1/Ti_2CO_2 (M = Fe, Co, Ni, Cu–Ru, Rh, Pd, Ag–O_s, Ir, Pt, Au) using density functional theory.[88] It was found

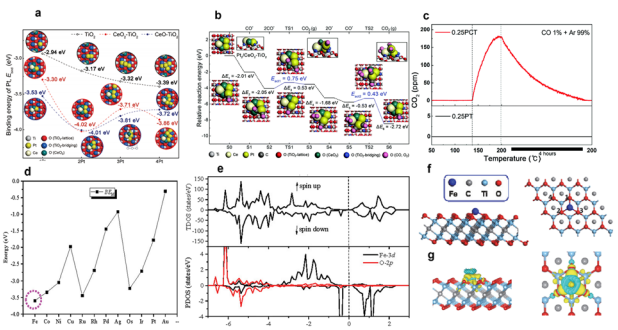

Fig. 5 (a) DFT calculation of the binding tendency of Pt SA to fully oxidized or reduced Ce ions at a CeO_x–TiO_2 interface; (b) Mars–van Krevelen-type CO oxidation pathway catalyzed by Pt_2 clusters fixed at the CeO_x–TiO_2 interface; (c) Results of CO-TPR analysis for 0.25 PT and 0.25 PCT catalysts. Reprinted with permission from ref. 87. Copyright 2022, The Royal Society of Chemistry; (d–g) DFT calculation of the binding energy PDOS diagram and PEDD diagram of metal (M) monoatom in M_1/TiC_2O_2. Reprinted with permission from ref. 88. Copyright 2020, Elsevier.

that an Fe_1/Ti_2CO_2 SAC showed excellent catalytic performance for CO oxidation at low temperatures. The adsorption of O_2 and CO on the Fe_1 atom of Fe_1/Ti_2CO_2 was extremely favorable (Fig. 5d–g). This work guides the experimental synthesis of low-cost SACs for CO oxidation.

3.4 Other catalytic reactions

In addition to the above applications, high-loading SACs have also been applied in many other catalytic reactions, such as oxidative conversion of methane, organic synthesis, CO_2 reduction and other applications.[8,89,90] The advantages of high-loading SACs, such as improved atom dispersion, catalytic activity, and selectivity, make them valuable in a wide range of catalytic processes.

According to the International Energy Agency (IEA), the global emission of CO_2 from the burning of fossil fuels was estimated at 33.8 billion tons in 2022, 300 million tons more than the previous year. In order to reduce global CO_2 emissions, recycling of CO_2 is essential. High-loading SACs can play a role in CO_2RR by improving the activity, selectivity, and stability of the catalyst. SACs can offer precise control over the reaction intermediates, allowing for the production of specific products, such as hydrocarbons or methanols. Converting CO_2 into methanol has high economic value. Fig. 6a shows the mechanism of photocatalytic CO_2 reduction to methanol. The reaction to produce methanol from CO_2 is a six-electron reduction process. Therefore, the photocatalyst activity is closely related to the localization of photogenerated electrons on the catalyst surface. Ma *et al.* loaded an ultra-high density of Co–N_2C single-atom active sites on a g-C_3N_4 photocatalyst, achieving a very high loading of 24.6 wt% (~6.2 at%).[91] Photocatalytic tests showed a methanol generation rate of 941 μmol g^{-1} over 4 h, which is 13.4 and 2.2 times higher than pure phase g-C_3N_4 (17.7 μmol g^{-1}) and CoO_x/g-C_3N_4-0.2 (423.9 μmol g^{-1}), respectively. In addition, the photocatalytic activity of the Co/g-C_3N_4-0.2 SAC did not decrease significantly after 12 cycles (~48 h). Besides being able to convert CO_2 into methanol, reducing it to commercial carbon monoxide is also a good choice. Zhao *et al.* used a general cascade anchoring strategy for the mass production of a series of M–NC SACs with a metal loading up to 12.1 wt%.[38] Among them, the Ni–NC SAC exhibited the potential for CO_2 reduction to CO and showed an 89% Faraday efficiency at −0.85 V with 30 mA cm^{-2} current density for CO.

After identify SACs with high activity for a particular reaction, large-scale preparation becomes the next challenge to address. Wang *et al.* successfully synthesized a series of high-loading SACs (up to 30 wt%) by pyrolyzing a metal coordination polymer at high temperatures.[90] This method is also suitable for large-scale synthesis of a series of multi-species metal SACs such as Ni, Cu, Zn, Ru, Rh, Pd, Pt, and Ir (Fig. 6b). The monatomic catalysts synthesized by this method all have extremely high metal loadings, such as 21.57 wt%/~5.30 at% (Ni), 22.36 wt%/~5.12 at% (Cu), 21.09 wt%/~4.70 at% (Zn), 13.47 wt%/~1.82 at% (Ru), 3.5 wt%/~0.42 at% (Rh), 3.8 wt%/~0.44 at% (Pd), 3.2 wt%/~0.20 at% (Pt), and 4.4 wt%/~0.29 at% (Ir). The SACs obtained by this synthesis method possessed excellent catalytic properties. It can be seen from Fig. 6c and d that the prepared Fe SAC demonstrated excellent properties (64% yield within 3 h, 89% selectivity) and high stability (almost no change for five cycles) in the styrene epoxide reaction.

In conclusion, high-loading SACs are now being widely used in photocatalysis, electrocatalysis and thermal catalysis.[92,93] It's important to note that while high-loading SACs can offer advantages in these applications, there may still be challenges to overcome, such as stability under harsh reaction conditions or the requirement for specific support materials. Further research and development efforts are ongoing to optimize the design, synthesis, and utilization of high-loading SACs in different catalytic reactions. We hope that high-loading SACs will find end use in the chemical industry and energy sector.

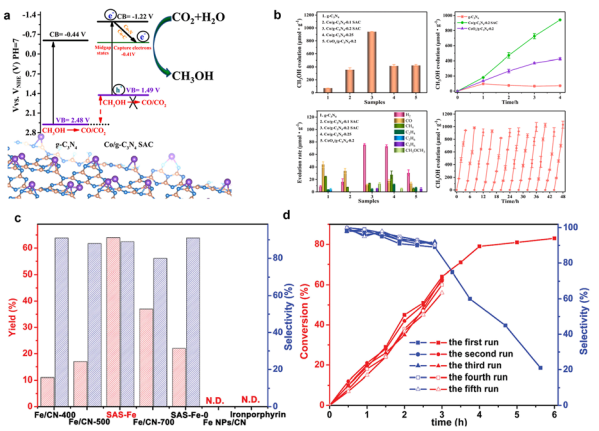

Fig. 6 (a) Diagram of photocatalytic CO_2 reduction to form methanol; (b) Photocatalytic CO_2 activity test for methanol production. Reprinted with permission from ref. 91. Copyright 2023, Elsevier; (c and d) Styrene epoxidation performance of high-loading Fe SACs. Reprinted with permission from ref. 90. Copyright 2022, Wiley-VCH GmbH.

4 Summary and outlook

This article summarizes recent advances in the synthesis and application of high-loading SACs, highlighting ways in which the electronic structure of the catalysts, active site density, and ultimately catalytic activity can be improved by maximizing the metal atom loading.[94] Thereafter, we explored applications of high-loading SACs in different catalytic reactions, including the ORR, water electrolysis, photocatalytic hydrogen production, CO oxidation reaction, and other catalytic reactions. Although SACs have now been studied for more than a decade, and remarkable recent progress has been made in the field, many challenges still need to be overcome before they find widespread application in the chemical industry or the energy sector.[95–97] The controlled preparation of SACs with high loading still presents significant challenges.[98,99] Particular issues that need to be resolved include:

i. The best way to describe the SAC loading has been disputed for a long time. Most of the scholars prefer to report metal loadings in SACs as a weight percentage (wt%). However, atom percentage (at%) actually depicts the number of single atomic active sites in SACs much more accurately (since at a fixed at% of metal, the wt% value will increase with the atomic number of the metal atoms which can lead to confusion). Therefore, at% should be the better indicator when comparing SAC loadings for a particular type of support.[100–103] Alternatively, mass activity could be used to compare metal SACs in terms of their catalytic properties, which is particularly useful when comparing SACs and metal nanoparticle catalysts.

ii. Although many strategies have been discovered to prevent the agglomeration of single atoms during the preparation of high-loading SACs, aggregation of atoms is inevitable above certain threshold loadings. It is hoped in the future that even more effective strategies can be found to prevent agglomeration from happening.

iii. Although many methods have been found to synthesize high-loading SACs, often these methods make it difficult to prepare catalysts in large quantities. Universal methods for the large-scale and controlled preparation of SACs with high single atom site densities are urgently needed. Such universal methods are key to the industrial scale preparation of SACs with high loadings.

iv. The majority of SACs reported to date with high loadings are of the type M_1–N–C (metal single atoms on N-doped carbons). For SACs based on oxide supports, metal loadings are typically much lower than M_1–N–C catalysts, limiting the range of application of SACs in catalysis and other applications. More work needs to be directed towards SACs based on other supports (metal oxides, metal nitrides, metal carbides, metal sulfides, *etc.*).

v. When analyzing the industrialization prospect of different methods for preparing SACs, several factors need to be considered, including cost, scalability, performance, and market demand. Considering that, wet chemistry methods currently appear to have great industrialization prospect because they are relatively cost-effective and can be easily scaled up for mass production. However, the loading of SACs prepared by this method is restricted. Studies concerning this are still relatively rare. In the actual research and application, the pyrolysis method to produce high loads of single atoms still occupies a dominant position, but it is hoped that a mild and controllable wet chemical method can be developed in the future.

Conflicts of interest

There are no conflicts to declare.

Acknowledgements

The work was supported by the National Natural Science Foundation of China (No. 92061125, 22209186), Beijing Natural Science Foundation (No. Z200012), Jiangxi Natural Science Foundation (No. 20212ACB213009, 20223BBG74004), and Youth Innovation Promotion Association, CAS (No. 2023343). GINW acknowledges funding support from the Royal Society Te Apārangi (for the award of a James Cook Research Fellowship) and Greg and Kathryn Trounson (for a generous philanthropic donation).

References

1 Z. Zhang, C. Feng, C. Liu, M. Zuo, L. Qin, X. Yan, Y. Xing, H. Li, R. Si, S. Zhou and J. Zeng, Electrochemical deposition as a universal route for fabricating single-atom catalysts, *Nat. Commun.*, 2020, **11**, 1–8.
2 S. K. Kaiser, Z. Chen, D. Faust Akl, S. Mitchell and J. Pérez-Ramírez, Single-atom catalysts across the periodic table, *Chem. Rev.*, 2020, **120**, 11703–11809.
3 Z. Li, S. Ji, Y. Liu, X. Cao, S. Tian, Y. Chen, Z. Niu and Y. Li, Well-defined materials for heterogeneous catalysis: from nanoparticles to isolated single-atom sites, *Chem. Rev.*, 2019, **120**, 623–682.
4 X. Sui, L. Zhang, J. Li, K. Doyle-Davis, R. Li, Z. Wang and X. Sun, Advanced support materials and interactions for atomically dispersed noble-metal catalysts: from support effects to design strategies, *Adv. Energy Mater.*, 2022, **12**, 2102556.
5 H. Xu, Y. Zhao, Q. Wang, G. He and H. Chen, Supports promote single-atom catalysts toward advanced electrocatalysis, *Coord. Chem. Rev.*, 2022, **451**, 214261.
6 B. Qiao, A. Wang, X. Yang, L. F. Allard, Z. Jiang, Y. Cui, J. Liu, J. Li and T. Zhang, Single-atom catalysis of CO oxidation using Pt_1/FeO_x, *Nat. Chem.*, 2011, **3**, 634–641.
7 L. Zhang, M. Zhou, A. Wang and T. Zhang, Selective hydrogenation over supported metal catalysts: From nanoparticles to single atoms, *Chem. Rev.*, 2019, **120**, 683–733.
8 W. Zhang, Y. Chao, W. Zhang, J. Zhou, F. Lv, K. Wang, F. Lin, H. Luo, J. Li, M. Tong, E. Wang and S. Guo, Emerging dual-atomic-site catalysts for efficient energy catalysis, *Adv. Mater.*, 2021, **33**, 2102576.
9 H. Xiong, A. K. Datye and Y. Wang, Thermally stable single-atom heterogeneous catalysts, *Adv. Mater.*, 2021, **33**, 2004319.
10 Y. Wang, H. Su, Y. He, L. Li, S. Zhu, H. Shen, P. Xie, X. Fu, G. Zhou, C. Feng, D. Zhao, F. Xiao, X. Zhu, Y. Zeng, M. Shao, S. Chen, G. Wu, J. Zeng and C. Wang, Advanced electrocatalysts with single-metal-atom active sites, *Chem. Rev.*, 2020, **120**, 12217–12314.
11 A. Wang, J. Li and T. Zhang, Heterogeneous single-atom catalysis, *Nat. Rev. Chem.*, 2018, **2**, 65–81.
12 S. K. Kaiser, I. Surin, A. Amorós-Pérez, S. Büchele, F. Krumeich, A. H. Clark, M. C. Román-Martínez, M. A. Lillo-Ródenas and J. Pérez-Ramírez, Design of carbon supports for metal-catalyzed acetylene hydrochlorination, *Nat. Commun.*, 2021, **12**, 4016.
13 D. Yu, Y. Ma, F. Hu, C. C. Lin, L. Li, H. Y. Chen, X. Han and S. Peng, Dual-sites coordination engineering of single atom

catalysts for flexible metal-air batteries, *Adv. Energy Mater.*, 2021, **11**, 2101242.

14 P. Rao, Y. Deng, W. Fan, J. Luo, P. Deng, J. Li, Y. Shen and X. Tian, Movable type printing method to synthesize high-entropy single-atom catalysts, *Nat. Commun.*, 2022, **13**, 5071.

15 Y. Pan, X. Wang, W. Zhang, L. Tang, Z. Mu, C. Liu, B. Tian, M. Fei, Y. Sun, H. Su, L. Gao, P. Wang, X. Duan, J. Ma and M. Ding, Boosting the performance of single-atom catalysts via external electric field polarization, *Nat. Commun.*, 2022, **13**, 3063.

16 X. Hai, S. Xi, S. Mitchell, K. Harrath, H. Xu, D. F. Akl, D. Kong, J. Li, Z. Li, T. Sun, H. Yang, Y. Cui, C. Su, X. Zhao, J. Li, J. Pérez-Ramírez and J. Lu, Scalable two-step annealing method for preparing ultra-high-density single-atom catalyst libraries, *Nat. Nanotechnol.*, 2022, **17**, 174–181.

17 L. Han, H. Cheng, W. Liu, H. Li, P. Ou, R. Lin, H.-T. Wang, C.-W. Pao, A. R. Head, C.-H. Wang, X. Tong, C.-J. Sun, W.-F. Pong, J. Luo, J.-C. Zheng and H. L. Xin, A single-atom library for guided monometallic and concentration-complex multimetallic designs, *Nat. Mater.*, 2022, **21**, 681–688.

18 W. Guo, Z. Wang, X. Wang and Y. Wu, General design concept for single-atom catalysts toward heterogeneous catalysis, *Adv. Mater.*, 2021, **33**, 2004287.

19 R. Qin, K. Liu, Q. Wu and N. Zheng, Surface coordination chemistry of atomically dispersed metal catalysts, *Chem. Rev.*, 2020, **120**, 11810–11899.

20 J. Xing, J. F. Chen, Y. H. Li, W. T. Yuan, Y. Zhou, L. R. Zheng, H. F. Wang, P. Hu, Y. Wang, H. J. Zhao, Y. Wang and H. G. Yang, Stable isolated metal atoms as active sites for photocatalytic hydrogen evolution, *Chem. – Eur. J.*, 2014, **20**, 2138–2144.

21 H. Wei, X. Liu, A. Wang, L. Zhang, B. Qiao, X. Yang, Y. Huang, S. Miao, J. Liu and T. Zhang, FeO_x-supported platinum single-atom and pseudo-single-atom catalysts for chemoselective hydrogenation of functionalized nitroarenes, *Nat. Commun.*, 2014, **5**, 1–8.

22 Y. J. Sa, D.-J. Seo, J. Woo, J. T. Lim, J. Y. Cheon, S. Y. Yang, J. M. Lee, D. Kang, T. J. Shin, H. S. Shin, H. Y. Jeong, C. S. Kim, M. G. Kim, T.-Y. Kim and S. H. Joo, A general approach to preferential formation of active Fe–Nx sites in Fe–N/C electrocatalysts for efficient oxygen reduction reaction, *J. Am. Chem. Soc.*, 2016, **138**, 15046–15056.

23 J. Amsler, B. B. Sarma, G. Agostini, G. Prieto, P. N. Plessow and F. Studt, Prospects of heterogeneous hydroformylation with supported single atom catalysts, *J. Am. Chem. Soc.*, 2020, **142**, 5087–5096.

24 J. Shan, J. Liao, C. Ye, J. Dong, Y. Zheng and S. Z. Qiao, The dynamic formation from metal-organic frameworks of high-density platinum single-atom catalysts with metal-metal interactions, *Angew. Chem., Int. Ed.*, 2022, **134**, e202213412.

25 J. Shan, C. Ye, Y. Jiang, M. Jaroniec, Y. Zheng and S.-Z. Qiao, Metal-metal interactions in correlated single-atom catalysts, *Sci. Adv.*, 2022, **8**, eabo0762.

26 K. Jiang, S. Back, A. J. Akey, C. Xia, Y. Hu, W. Liang, D. Schaak, E. Stavitski, J. K. Nørskov, S. Siahrostami and H. Wang, Highly selective oxygen reduction to hydrogen peroxide on transition metal single atom coordination, *Nat. Commun.*, 2019, **10**, 1–11.

27 Z. Du, X. Chen, W. Hu, C. Chuang, S. Xie, A. Hu, W. Yan, X. Kong, X. Wu, H. Ji and L.-J. Wan, Cobalt in nitrogen-doped graphene as single-atom catalyst for high-sulfur content lithium–sulfur batteries, *J. Am. Chem. Soc.*, 2019, **141**, 3977–3985.

28 K. Wang, X. Wang and X. Liang, Synthesis of high metal loading single atom catalysts and exploration of the active center structure, *ChemCatChem*, 2021, **13**, 28–58.

29 J. Fu, J. Dong, R. Si, K. Sun, J. Zhang, M. Li, N. Yu, B. Zhang, M. G. Humphrey, Q. Fu and J. Huang, Synergistic effects for enhanced catalysis in a dual single-atom catalyst, *ACS Catal.*, 2021, **11**, 1952–1961.

30 J. Yang, W. Li, D. Wang and Y. Li, Electronic metal–support interaction of single-atom catalysts and applications in electrocatalysis, *Adv. Mater.*, 2020, **32**, 2003300.

31 L. Wang, M.-X. Chen, Q.-Q. Yan, S.-L. Xu, S.-Q. Chu, P. Chen, Y. Lin and H.-W. Liang, A sulfur-tethering synthesis strategy toward high-loading atomically dispersed noble metal catalysts, *Sci. Adv.*, 2019, **5**, eaax6322.

32 C. Xia, Y. Qiu, Y. Xia, P. Zhu, G. King, X. Zhang, Z. Wu, J. Y. T. Kim, D. A. Cullen, D. Zheng, P. Li, M. Shakouri, E. Heredia, P. Cui, H. N. Alshareef, Y. Hu and H. Wang, General synthesis of single-atom catalysts with high metal loading using graphene quantum dots, *Nat. Chem.*, 2021, **13**, 887–894.

33 Z. Zeng, Y. Su, X. Quan, W. Choi, G. Zhang, N. Liu, B. Kim, S. Chen, H. Yu and S. Zhang, Single-atom platinum confined by the interlayer nanospace of carbon nitride for efficient photocatalytic hydrogen evolution, *Nano Energy*, 2020, **69**, 104409.

34 Q. Zuo, T. Liu, C. Chen, Y. Ji, X. Gong, Y. Mai and Y. Zhou, Ultrathin metal-organic framework nanosheets with ultrahigh loading of single Pt atoms for efficient visible-light-driven photocatalytic H_2 evolution, *Angew. Chem., Int. Ed.*, 2019, **58**, 10198–10203.

35 D. Cao, Z. Zhang, Y. Cui, R. Zhang, L. Zhang, J. Zeng and D. Cheng, One-step approach for constructing high-density single-atom catalysts toward overall water splitting at industrial current densities, *Angew. Chem., Int. Ed.*, 2023, **135**, e202214259.

36 Z. Wang, S.-M. Xu, Y. Xu, L. Tan, X. Wang, Y. Zhao, H. Duan and Y.-F. Song, Single Ru atoms with precise coordination on a monolayer layered double hydroxide for efficient electrooxidation catalysis, *Chem. Sci.*, 2019, **10**, 378–384.

37 F. Li, G.-F. Han, H.-J. Noh, S.-J. Kim, Y. Lu, H. Y. Jeong, Z. Fu and J.-B. Baek, Boosting oxygen reduction catalysis with abundant copper single atom active sites, *Energy Environ. Sci.*, 2018, **11**, 2263–2269.

38 L. Zhao, Y. Zhang, L.-B. Huang, X.-Z. Liu, Q.-H. Zhang, C. He, Z.-Y. Wu, L.-J. Zhang, J. Wu, W. Yang, L. Gu, J.-S. Hu and L.-J. Wan, Cascade anchoring strategy for general mass production of high-loading single-atomic metal-nitrogen catalysts, *Nat. Commun.*, 2019, **10**, 1–11.

39 L. Han, X. Liu, J. Chen, R. Lin, H. Liu, F. Lü, S. Bak, Z. Liang, S. Zhao, E. Stavitski, J. Luo, R. R. Adzic and H. L.

Xin, Atomically dispersed molybdenum catalysts for efficient ambient nitrogen fixation, *Angew. Chem., Int. Ed.*, 2019, **58**, 2525.

40 Y. Cheng, S. He, S. Lu, J. P. Veder, B. Johannessen, L. Thomsen, M. Saunders, T. Becker, R. De Marco, Q. Li, S.-z. Yang and S. P. Jiang, Iron single atoms on graphene as nonprecious metal catalysts for high-temperature polymer electrolyte membrane fuel cells, *Adv. Sci.*, 2019, **6**, 1802066.

41 S. An, G. Zhang, T. Wang, W. Zhang, K. Li, C. Song, J. T. Miller, S. Miao, J. Wang and X. Guo, High-density ultra-small clusters and single-atom Fe sites embedded in graphitic carbon nitride ($g\text{-}C_3N_4$) for highly efficient catalytic advanced oxidation processes, *ACS Nano*, 2018, **12**, 9441–9450.

42 X. Zhang, C. Li, X. Wang, S. Yang, Y. Tan, F. Yuan, S. Zheng, D. D. Dionysiou and Z. Sun, Defect engineering modulated iron single atoms with assist of layered clay for enhanced advanced oxidation processes, *Small*, 2022, **18**, 2204793.

43 X. Wu, Q. Wang, S. Yang, J. Zhang, Y. Cheng, H. Tang, L. Ma, X. Min, C. Tang, S. P. Jiang, F. Wu, Y. Lei, S. Ciampic, S. Wang and L. Dai, Sublayer-enhanced atomic sites of single atom catalysts through in situ atomization of metal oxide nanoparticles, *Energy Environ. Sci.*, 2022, **15**, 1183–1191.

44 A. Mehmood, M. Gong, F. Jaouen, A. Roy, A. Zitolo, A. Khan, M.-T. Sougrati, M. Primbs, A. M. Bonastre, D. Fongalland, G. Drazic, P. Strasser and A. Kucernak, High loading of single atomic iron sites in Fe–NC oxygen reduction catalysts for proton exchange membrane fuel cells, *Nat. Catal.*, 2022, **5**, 311–323.

45 H. Yang, L. Shang, Q. Zhang, R. Shi, G. I. N. Waterhouse, L. Gu and T. Zhang, A universal ligand mediated method for large scale synthesis of transition metal single atom catalysts, *Nat. Commun.*, 2019, **10**, 1–9.

46 S. Zhao, Y. Cheng, J.-P. Veder, B. Johannessen, M. Saunders, L. Zhang, C. Liu, M. F. Chisholm, R. De Marco, J. Liu, S.-Z. Yang and S. P. Jiang, One-pot pyrolysis method to fabricate carbon nanotube supported Ni single-atom catalysts with ultrahigh loading, *ACS Appl. Energy Mater.*, 2018, **1**, 5286–5297.

47 J. Li, S. Chen, N. Yang, M. Deng, S. Ibraheem, J. Deng, J. Li, L. Li and Z. Wei, Ultrahigh-loading zinc single-atom catalyst for highly efficient oxygen reduction in both acidic and alkaline media, *Angew. Chem., Int. Ed.*, 2019, **58**, 7035–7039.

48 H. Wang, X. Li, Y. Jiang, M. Li, Q. Xiao, T. Zhao, S. Yang, C. Qi, P. Qiu, J. Yang, Z. Jiang and W. Luo, A universal single-atom coating strategy based on tannic acid chemistry for multifunctional heterogeneous catalysis, *Angew. Chem., Int. Ed.*, 2022, **134**, e202200465.

49 L. Xing, Y. Jin, Y. Weng, R. Feng, Y. Ji, H. Gao, X. Chen, X. Zhang, D. Jia and G. Wang, Top-down synthetic strategies toward single atoms on the rise, *Matter*, 2022, **5**, 788–807.

50 A. Beniya and S. Higashi, Towards dense single-atom catalysts for future automotive applications, *Nat. Catal.*, 2019, **2**, 590–602.

51 S. Ji, Y. Chen, X. Wang, Z. Zhang, D. Wang and Y. Li, Chemical synthesis of single atomic site catalysts, *Chem. Rev.*, 2020, **120**, 11900–11955.

52 T. Ma, H. Cao, S. Li, S. Cao, Z. Zhao, Z. Wu, R. Yan, C. Yang, Y. Wang, P. A. van Aken, L. Qiu, Y.-G. Wang and C. Cheng, Crystalline lattice-confined atomic Pt in metal carbides to match electronic structures and hydrogen evolution behaviors of platinum, *Adv. Mater.*, 2022, **34**, 2206368.

53 R. Li and D. Wang, Superiority of dual-atom catalysts in electrocatalysis: one step further than single-atom catalysts, *Adv. Energy Mater.*, 2022, **12**, 2103564.

54 Y. Cheng, S. Zhao, H. Li, S. He, J.-P. Veder, B. Johannessen, J. Xiao, S. Lu, J. Pan, M. F. Chisholm, S.-Z. Yang, C. Liu, J. G. Chen and S. P. Jiang, Unsaturated edge-anchored Ni single atoms on porous microwave exfoliated graphene oxide for electrochemical CO_2, *Appl. Catal., B*, 2019, **243**, 294–303.

55 Q. Dong, S. Ma, J. Zhu, F. Yue, Y. Geng, J. Zheng, Y. Ge, C. Fan, H. Zhang, M. Xiang and Q. Zhu, Ultrahigh mass activity for the hydrogen evolution reaction by anchoring platinum single atoms on active {100} facets of TiC via cation defect engineering, *Adv. Funct. Mater.*, 2022, 2210665.

56 C. Xu, J. Wu, L. Chen, Y. Gong, B. Mao, J. Zhang, J. Deng, M. Mao, Y. Shi, Z. Hou, M. Cao, H. Li, H. Zhou, Z. Huang and Y. Kuang, Boric acid–assisted pyrolysis for high–loading single–atom catalysts to boost oxygen reduction reaction in Zn–air batteries, *Energy Environ. Mater.*, 2023, e12569.

57 Y. Xiong, W. Sun, Y. Han, P. Xin, X. Zheng, W. Yan, J. Dong, J. Zhang, D. Wang and Y. Li, Cobalt single atom site catalysts with ultrahigh metal loading for enhanced aerobic oxidation of ethylbenzene, *Nano Res.*, 2021, **14**, 2418–2423.

58 H. Zhou, Y. Zhao, J. Gan, J. Xu, Y. Wang, H. Lv, S. Fang, Z. Wang, Z. Deng, X. Wang, P. Liu, W. Guo, B. Mao, H. Wang, T. Yao, X. Hong, S. Wei, X. Duan, J. Luo and Y. Wu, Cation-exchange induced precise regulation of single copper site triggers room-temperature oxidation of benzene, *J. Am. Chem. Soc.*, 2020, **142**, 12643–12650.

59 R. Lang, W. Xi, J.-C. Liu, Y.-T. Cui, T. Li, A. F. Lee, F. Chen, Y. Chen, L. Li, L. Li, J. Lin, S. Miao, X. Liu, A.-Q. Wang, X. Wang, J. Luo, B. Qiao, J. Li and T. Zhang, Non defect-stabilized thermally stable single-atom catalyst, *Nat. Commun.*, 2019, **10**, 234.

60 M. Leskelä and M. Ritala, Atomic layer deposition (ALD): From precursors to thin film structures, *Thin Solid Films*, 2002, **409**, 138–146.

61 J. Lu, J. W. Elam and P. C. Stair, Synthesis and stabilization of supported metal catalysts by atomic layer deposition, *Acc. Chem. Res.*, 2013, **46**, 1806–1815.

62 J. Lu, J. W. Elam and P. C. Stair, Atomic layer deposition-Sequential self-limiting surface reactions for advanced catalyst "bottom-up" synthesis, *Surf. Sci. Rep.*, 2016, **71**, 410–472.

63 J. Fonseca and J. Lu, Single-atom catalysts designed and prepared by the atomic layer deposition technique, *ACS Catal.*, 2021, **11**, 7018–7059.
64 S. Sun, G. Zhang, N. Gauquelin, N. Chen, J. Zhou, S. Yang, W. Chen, X. Meng, D. Geng, M. N. Banis, R. Li, S. Ye, S. Knights, G. A. Botton, T.-K. Sham and X. Sun, Single-atom catalysis using Pt/graphene achieved through atomic layer deposition, *Sci. Rep.*, 2013, **3**, 1775.
65 J. Gu, M. Jian, L. Huang, Z. Sun, A. Li, Y. Pan, J. Yang, W. Wen, W. Zhou, Y. Lin, H.-J. Wang, X. Liu, L. Wang, X. Shi, X. Huang, L. Cao, S. Chen, X. Zheng, H. Pan, J. Zhu, S. Wei, W.-X. Li and J. Lu, Synergizing metal–support interactions and spatial confinement boosts dynamics of atomic nickel for hydrogenations, *Nat. Nanotechnol.*, 2021, **16**, 1141–1149.
66 M. Tavakkoli, N. Holmberg, R. Kronberg, H. Jiang, J. Sainio, E. I. Kauppinen, T. Kallio and K. Laasonen, Electrochemical activation of single-walled carbon nanotubes with pseudo-atomic-scale platinum for the hydrogen evolution reaction, *ACS Catal.*, 2017, **7**, 3121–3130.
67 L. Zhang, L. Han, H. Liu, X. Liu and J. Luo, Potential-cycling synthesis of single platinum atoms for efficient hydrogen evolution in neutral media, *Angew. Chem., Int. Ed.*, 2017, **129**, 13882–13886.
68 Z. Zhang, C. Feng, C. Liu, M. Zuo, L. Qin, X. Yan, Y. Xing, H. Li, R. Si, S. Zhou and J. Zeng, Electrochemical deposition as a universal route for fabricating single-atom catalysts, *Nat. Commun.*, 2020, **11**, 1215.
69 C.-X. Zhao, J.-N. Liu, J. Wang, C. Wang, X. Guo, X.-Y. Li, X. Chen, L. Song, B.-Q. Li and Q. Zhang, A clicking confinement strategy to fabricate transition metal single-atom sites for bifunctional oxygen electrocatalysis, *Sci. Adv.*, 2022, **8**, eabn5091.
70 J. Wu, L. Xiong, B. Zhao, M. Liu and L. Huang, Densely populated single atom catalysts, *Small Methods*, 2020, **4**, 1900540.
71 M. Liu, Z. Zhao, X. Duan and Y. Huang, Nanoscale structure design for high-performance Pt-based ORR catalysts, *Adv. Mater.*, 2019, **31**, 1802234.
72 Z. Li, B. Li, Y. Hu, S. Wang and C. Yu, Highly-dispersed and high-metal-density electrocatalysts on carbon supports for the oxygen reduction reaction: from nanoparticles to atomic-level architectures, *Mater. Adv.*, 2022, **3**, 779–809.
73 L. Zou, Y. S. Wei, C. C. Hou, C. Li and Q. Xu, Single-atom catalysts derived from metal–organic frameworks for electrochemical applications, *Small*, 2021, **17**, 2004809.
74 Z. Jin, P. Li, Y. Meng, Z. Fang, D. Xiao and G. Yu, Understanding the inter-site distance effect in single-atom catalysts for oxygen electroreduction, *Nat. Catal.*, 2021, **4**, 615–622.
75 A. Kulkarni, S. Siahrostami, A. Patel and J. K. Nørskov, Understanding catalytic activity trends in the oxygen reduction reaction, *Chem. Rev.*, 2018, **118**, 2302–2312.
76 L. Zhang, T. Yang, W. Zang, Z. Kou, Y. Ma, M. Waqar, X. Liu, L. Zheng, S. J. Pennycook, Z. Liu, X. J. Loh, L. Shen and J. Wang, Quasi-paired Pt atomic sites on Mo_2C promoting selective four-electron oxygen reduction, *Adv. Sci.*, 2021, **8**, 2101344.
77 T. Li, J. Liu, Y. Song and F. Wang, Photochemical solid-phase synthesis of platinum single atoms on nitrogen-doped carbon with high loading as bifunctional catalysts for hydrogen evolution and oxygen reduction reactions, *ACS Catal.*, 2018, **8**, 8450–8458.
78 W.-H. Li, J. Yang, H. Jing, J. Zhang, Y. Wang, J. Li, J. Zhao, D. Wang and Y. Li, Creating high regioselectivity by electronic metal–support interaction of a single-atomic-site catalyst, *J. Am. Chem. Soc.*, 2021, **143**, 15453–15461.
79 B. Chu, Q. Ma, Z. Li, B. Li, F. Huang, Q. Pang, Y. Chen, B. Li and J. Z. Zhang, Design and preparation of three-dimensional hetero-electrocatalysts of NiCo-layered double hydroxide nanosheets incorporated with silver nanoclusters for enhanced oxygen evolution reactions, *Nanoscale*, 2021, **13**, 11150–11160.
80 T. Zhang, Single-atom catalysis: Far beyond the matter of metal dispersion, *Nano Lett.*, 2021, **21**, 9835–9837.
81 X. Chen, J. Wan, J. Wang, Q. Zhang, L. Gu, L. Zheng, N. Wang and R. Yu, Atomically dispersed ruthenium on nickel hydroxide ultrathin nanoribbons for highly efficient hydrogen evolution reaction in alkaline media, *Adv. Mater.*, 2021, **33**, 2104764.
82 J. Zhou, J. Pan, Y. Jin, Z. Peng, Z. Xu, Q. Chen, P. Ren, X. Zhou and K. Wu, Single-cation catalyst: Ni cation in monolayered CuO for CO oxidation, *J. Am. Chem. Soc.*, 2022, **144**, 8430–8433.
83 S. Yu, D. Kim, Z. Qi, S. Louisia, Y. Li, G. A. Somorjai and P. Yang, Nanoparticle assembly induced ligand interactions for enhanced electrocatalytic CO_2 conversion, *J. Am. Chem. Soc.*, 2021, **143**, 19919–19927.
84 Y. Lu, J. Wang, L. Yu, L. Kovarik, X. Zhang, A. S. Hoffman, A. Gallo, S. R. Bare, D. Sokaras, T. Kroll, V. Dagle, H. Xin and A. M. Karim, Identification of the active complex for CO oxidation over single-atom Ir-on-$MgAl_2O_4$ catalysts, *Nat. Catal.*, 2019, **2**, 149–156.
85 V. Muravev, G. Spezzati, Y.-Q. Su, A. Parastaev, F.-K. Chiang, A. Longo, C. Escudero, N. Kosinov and E. J. Hensen, Interface dynamics of Pd–CeO_2 single-atom catalysts during CO oxidation, *Nat. Catal.*, 2021, **4**, 469–478.
86 P. Jing, X. Gong, B. Liu and J. Zhang, Recent advances in synergistic effect promoted catalysts for preferential oxidation of carbon monoxide, *Catal. Sci. Technol.*, 2020, **10**, 919–934.
87 M. Yoo, Y.-S. Yu, H. Ha, S. Lee, J.-S. Choi, S. Oh, E. Kang, H. Choi, H. An, K.-S. Lee, J. Y. Park, R. Celestre, M. A. Marcus, K. Nowrouzi, D. Taube, D. A. Shapiro, W. Jung, C. Kim and H. Y. Kim, A tailored oxide interface creates dense Pt single-atom catalysts with high catalytic activity, *Energy Environ. Sci.*, 2020, **13**, 1231–1239.
88 C. Zhu, J.-X. Liang, Y.-G. Wang and J. Li, Non-noble metal single-atom catalyst with MXene support: Fe_1/Ti_2CO_2 for CO oxidation, *Chin. J. Catal.*, 2022, **43**, 1830–1841.
89 J. Li, L. Zhang, K. Doyle-Davis, R. Li and X. Sun, Recent advances and strategies in the stabilization of single-atom catalysts for electrochemical applications, *Carbon Energy*, 2020, **2**, 488–520.

90 Y. Xiong, W. Sun, P. Xin, W. Chen, X. Zheng, W. Yan, L. Zheng, J. Dong, J. Zhang, D. Wang and Y. Li, Gram-scale synthesis of high-loading single-atomic-site Fe catalysts for effective epoxidation of styrene, *Adv. Mater.*, 2020, **32**, 2000896.

91 M. Ma, Z. Huang, D. E. Doronkin, W. Fa, Z. Rao, Y. Zou, R. Wang, Y. Zhong, Y. Cao, R. Zhang and Y. Zhou, Ultrahigh surface density of Co-N_2C single-atom-sites for boosting photocatalytic CO_2 reduction to methanol, *Appl. Catal., B*, 2022, **300**, 120695.

92 M. Wang, L. Wang, Q. Li, D. Wang, L. Yang, Y. Han, Y. Ren, G. Tian, X. Zheng, M. Ji, C. Zhu, L. Peng and G. I. N. Waterhouse, Regulating the coordination geometry and oxidation state of single-atom Fe sites for enhanced oxygen reduction electrocatalysis, *Small*, 2023, **19**, 2300373.

93 X. Xie, L. Peng, H. Yang, G. I. N. Waterhouse, L. Shang and T. Zhang, MIL-101-derived mesoporous carbon supporting highly exposed Fe single-atom sites as efficient oxygen reduction reaction catalysts, *Adv. Mater.*, 2021, **33**, 2101038.

94 Q. Wang, Y. Yang, F. Sun, G. Chen, J. Wang, L. Peng, W. T. Chen, L. Shang, J. Zhao, D. Sun-Waterhouse, T. Zhang and G. I. N. Waterhouse, Molten NaCl-assisted synthesis of porous Fe-N-C electrocatalysts with a high density of catalytically accessible FeN_4 active sites and outstanding oxygen reduction reaction performance, *Adv. Energy Mater.*, 2021, **11**, 2100219.

95 M. Abbas and M. A. Z. G. Sial, New horizon in stabilization of single atoms on metal-oxide supports for CO_2 reduction, *Nano Mater. Sci.*, 2021, **3**, 368–389.

96 L. Peng, L. Shang, T. Zhang and G. I. N. Waterhouse, Recent advances in the development of single-atom catalysts for oxygen electrocatalysis and zinc–air batteries, *Adv. Energy Mater.*, 2020, **10**, 2003018.

97 Z. X. Mao, M. J. Wang, L. Liu, L. Peng, S. Chen, L. Li, J. Li and Z. Wei, $ZnCl_2$ salt facilitated preparation of FeNC: Enhancing the content of active species and their exposure for highly-efficient oxygen reduction reaction, *Chin. J. Catal.*, 2020, **41**, 799–806.

98 Z. Zhang, K. Chen, Q. Zhao, M. Huang and X. Ouyang, Electrocatalytic and photocatalytic performance of noble metal doped monolayer MoS_2 in the hydrogen evolution reaction: A first principles study, *Nano Mater. Sci.*, 2021, **3**, 89–94.

99 F. Wang, M. Hao, W. Liu, P. Yan, B. Fang, S. Li, J. Liang, M. Zhu and L. Cui, Low-cost fabrication of highly dispersed atomically-thin MoS_2 nanosheets with abundant active Mo-terminated edges, *Nano Mater. Sci.*, 2021, **3**, 205–212.

100 C. Lin, H. Zhang, X. Song, D.-H. Kim, X. Li, Z. Jiang and J.-H. Lee, 2D-organic framework confined metal single atoms with the loading reaching the theoretical limit, *Mater. Horiz.*, 2020, **7**, 2726–2733.

101 Y. Ma, Y. Ren, Y. Zhou, W. Liu, W. Baaziz, O. Ersen, C. Pham-Huu, M. Greiner, W. Chu, A. Wang, T. Zhang and Y. Liu, High-density and thermally stable palladium single-atom catalysts for chemoselective hydrogenations, *Angew. Chem., Int. Ed.*, 2020, **132**, 21797–21803.

102 T. Jing, T. Li, D. Rao, M. Wang and Y. ZuoDefining the loading of single-atom catalysts: Weight fraction or atomic fraction?, *Mater. Today Energy*, 2023, **31**, 101197.

103 H. Li, L. Wang, Y. Dai, Z. Pu, Z. Lao, Y. Chen, M. Wang, X. Zheng, J. Zhu, W. Zhang, R. Si, C. Ma and J. Zeng, Synergetic interaction between neighbouring platinum monomers in CO_2 hydrogenation, *Nat. Nanotechnol.*, 2018, **13**, 411–417.